Intermolecular Dynamics of Room-Temperature Ionic Liquids: Femtosecond Optical Kerr Effect Measurements on 1-Alkyl-3-methylimidazolium Bis((trifluoromethyl)sulfonyl)imides†

Byung-Ryool Hyun,‡ Sergei V. Dzyuba,‡ Richard A. Bartsch,‡ and Edward L. Quitevis*,‡,§

Departments of Chemistry and Biochemistry and of Physics, Texas Tech University, Lubbock, Texas 79409

Received: November 12, 2001; In Final Form: June 10, 2002

Using optically heterodyne-detected Raman-induced Kerr effect spectroscopy (OHD-RIKES) with 40 fs laser pulses, the transient birefringence in the room-temperature ionic liquids (RTILs), 1-alkyl-3-methylimidazolium bis((trifluoromethyl)sulfonyl)imides, $[C_n\text{mim}]NTf_2$ with $n = 2, 4, 5, 6, 8, 10$ (C2, C4, C5, C6, C8, C10), has been studied at room temperature and ambient pressure. Near zero delay, the OHD-RIKES response is dominated by the instantaneous electronic response. The nuclear response appears as a shoulder on the electronic response. Between 0 and 1 ps, the nuclear response is dominated by the intermolecular vibrational (nondiffusive) response. For C4, C5, C6, and C8, the 1/e time of the pseudo-exponential tail of the intermolecular response decreases with viscosity, in accord with the hydrodynamic model for vibrational dephasing. Superimposed on the OHD-RIKES response for C4, C5, and C6 is a coherent oscillation with a frequency of $\sim$140 cm^{-1}. The intermolecular vibrational spectra for these RTILs obtained from the reduced OHD-RIKES data by using a Fourier transform procedure extend from 0 to 200 cm^{-1} and are bimodal with a low-frequency component at $\sim$22 cm^{-1} and a high-frequency component at $\sim$84 cm^{-1}. The relative contribution of the high-frequency component to the total band increases in going from C2 to C5 and remains constant for C5, C6, and C8. The behavior of the reduced spectral densities is consistent with increasing order in the liquid. It is proposed that the 140 cm^{-1} oscillation arises from collective motions of locally ordered domains in the liquid.

I. Introduction

There is recently great interest in room-temperature ionic liquids (RTILs) because of their potential as "green" designer solvents for use in catalysis, chemical synthesis, separations, and as electrolytes in batteries and solar cells.[1−3] The choice of the RTIL can influence the outcome of a particular reaction or application. It is therefore important to fully characterize the properties of these materials in order to choose the right ionic liquid for a particular process. Most efforts to date have focused on bulk physical properties, such as phase transitions, viscosity, and density, and correlating these properties to the molecular structure of the ionic liquid.[4−10]

A complete understanding of the effect of ionic liquids on chemical reactions requires an understanding of the microscopic dynamics of these materials. Of particular interest is the effect of ionic liquids on charge transfer (CT) reactions. Because CT is strongly dependent on solvation dynamics, it is important to obtain information about the solvent response function and intermolecular modes of the ionic liquid.[11] By correlating the microscopic dynamics to the bulk physical properties of ionic liquids, one can better understand how to synthesize RTILs with properties precisely tailored for a particular chemical reaction.

RTILs are fluids composed entirely of ions. Their liquid-state dynamics are expected to be very complex because of the molecular structure of the ions and the nature of the intermolecular interactions. For simple ionic materials composed of monatomic ions, these interactions involve Coulombic forces between the charges, polarization, and dispersion effects.[12] Because the ions themselves will be influenced by neighboring ions, the interaction potentials for these liquids will inherently be many-body in character. The molecular structure of the ions in RTILs presents an additional complexity due to the possibility of interactions between specific functional groups on the ions. A complete understanding of the liquid dynamics in these materials will not be obtained from a single study but will require a multifaceted approach involving a variety of experimental and theoretical techniques.

A key to understanding the molecular dynamics of these materials is their liquid structure. Proton NMR measurements indicate that ionic liquids have a high degree of order.[7,13] Chemical shifts of the imidazolium ring protons are anion and concentration dependent.[7] This dependence can be explained by the formation of ion pairs between the imidazolium cation and the anion. Kinetic analysis of the photoelectron transfer from excited-state ruthenium(II) tris(bipyridyl), $*R^{2+}$, to methyl viologen, MV^{2+}, in $[C_4\text{mim}]PF_6$ is also consistent with the liquid being ordered.[14] The preexponential factor of the rate constant for the reaction between $*R^{2+}$ and MV^{2+} in the ionic liquid is extremely large for a bimolecular reaction. The large value of the preexponential factor is indicative of a large positive entropy of activation. Such a large value for the entropy of activation suggests that solvent ions are freed up on formation of the $[*R^{2+}\text{- - -}MV^{2+}]$ encounter complex. This in turn suggests that the ionic liquid is highly ordered. Further evidence for this ordered structure can be found in the dielectric spectroscopy of ionic liquids. For room temperature molten ethylammonium nitrate (EAN) in the normal fluid region, the extrapolated high-frequency permittivity is substantially higher than the square of the refractive index.[15] This dispersion step implies the

† Part of the special issue "G. Wilse Robinson Festschrift".

* To whom correspondence should be addressed. E-mail: edward.quitevis@ttu.edu. Fax: (806)742-1289.

‡ Department of Chemistry and Biochemistry.

§ Department of Physics.

10.1021/jp0141575 CCC: $22.00
Published on Web 07/24/2002

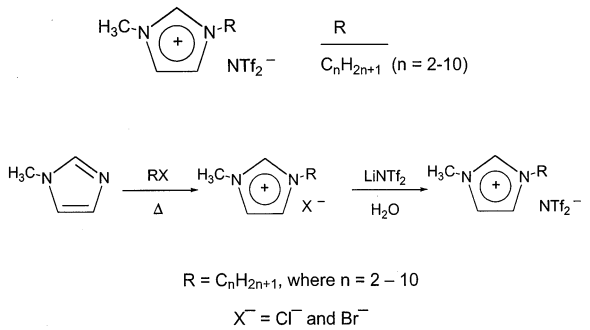

Figure 1. Structure of 1-alkyl-3-methylimidazolium bis((trifluoromethyl)sulfonyl)imides and synthetic scheme.

existence of a higher frequency regime of dispersion and dielectric loss. This additional contribution is thought to arise from vibrational modes associated with the relative motions of cation and anion lattices.

In this paper, we report the first application of optical heterodyne-detected Raman-induced Kerr effect spectroscopy (OHD-RIKES) to RTILs, specifically, the first direct measurement of the ultrafast dynamics of 1-alkyl-3-methylimidazolium bis((trifluoromethyl)sulfonyl)imides (bis(triflyl)imides), [$C_n$mim]-NTf_2 with $n = 2, 4, 5, 6, 8, 10$ (C2, C4, C5, C6, C8, C10) (Figure 1). The experiments were conducted at room temperature and ambient pressure with 40-fs pulses. OHD-RIKES is a nonlinear optical (NLO) technique that is widely used to study liquid-state dynamics. Theories have been developed that use the OHD-RIKES data to understand condensed-phase chemical dynamics. For example, the OHD-RIKES response of a liquid can be used to calculate a dipolar solvation-time correlation function that can be compared to the solvent response function obtained in time-dependent fluorescence Stokes shift (TDFSS measurements).[16] Alternatively, the OHD-RIKES response can be converted to a spectral density that gives the polarizability-weighted distribution of low-frequency modes in the liquid. The solvent response in excited-state CT as measured in TDFSS can be theoretically connected to the OHD-RIKES response by introducing a distribution of low-frequency oscillators to describe the ultrafast solvation dynamics.[17] Although intermolecular modes that determine the OHD-RIKES response are not necessarily the same as the ones that determine the solvent response in TDFSS, the spectral densities provide a rough approximation to the distribution of intermolecular modes of the solvent that couple to the reaction dynamics.[18]

This initial study is focused on determining the effect of varying the length of the alkyl chain on the ultrafast dynamics associated with the intermolecular modes of these ionic materials. This paper is organized as follows. In section II, brief descriptions of the synthesis and physical characterization of these materials and the OHD-RIKES apparatus and data acquisition are given. In section III, the OHD-RIKES data for these RTILs are presented. In section IV, the analysis of the temporal and frequency representations of the data is given. The reduced spectral densities obtained from the OHD-RIKES responses by using a Fourier transform procedure are analyzed in terms of a bimodal line shape function. The OHD-RIKES data are discussed in the context of the ordered structure of the liquid.

II. Experimental Methods

A. Synthesis and Physical Characterization. The synthesis and bulk physical measurements of these RTILs have been described previously.[10] For the synthesis of the RTILs, commercially available, reagent grade starting materials from Acros or Aldrich were used as received. The RTILs were prepared as shown in Figure 1. The precursor imidazolium halide was prepared by neat reactions of equivalent amounts of 1-methylimidazole and the appropriate alkyl bromide or chloride.[19] Without purification of the imidazolium halide, a metathesis reaction gave the NTf_2^--containing ionic liquids in high yield. The synthesis of the [$C_n$mim] salts was carried out by beginning with 10 mL of 1-methylimidazole. In several instances, the syntheses were also carried out on a larger scale with no apparent reduction in yield. The identity of the products was confirmed by elemental analysis by Desert Analytics Laboratory, Tucson, AZ, and by use of ^{1}H NMR and IR spectroscopy. Densities were measured by use of 1-mL pycnometers or an Anton-PARR Density Measurement System (DMA 602 density measuring cell and DMA 60 density meter with temperature control from a flow-through cooler and bath-circulator). Dynamic viscosities were measured with an Oswald viscometer. Table 1 summarizes the densities and viscosities of these RTILs.[10]

TABLE 1: Physical Properties of [$C_n$mim]NTf_2 Ionic Liquids at 25 °C[a,b]

liquid	ρ/g mL^{-1}	η/cP
C2	1.519	25
C4	1.436	44
C5	1.403	50
C6	1.372	59
C8	1.320	74
C10	1.271	90

[a] Reference 10. [b] ρ = density; η = viscosity.

B. OHD-RIKES Apparatus. Although some changes have been made to the femtosecond Ti:sapphire laser and the OHD-RIKES setup since the previously published work,[20−22] the apparatus employed in these experiments is basically the same. Linearly polarized ~40 fs optical pulses centered at ~800 nm were generated via Kerr-lens mode-locking of a home-built continuous wave Ti:sapphire laser pumped by an all-lines Coherent Innova 90C Ar^+ laser.[23] Stable mode-locking at a repetition rate of 87 MHz was obtained with 4.2 W of laser pump power. To compensate for group-velocity dispersion of the output coupler and the pump−probe optics, the output of the Ti:sapphire laser was directed into a pair of fused silica prisms in a near retro-reflecting geometry.

The laser pulses were split into two beams using a 50%/50% near-IR 5-μm pellicle beam splitter. The beams were then sent through two separate arms of a Michelson interferometer. Each beam was passed through an achromatic quartz zeroth-order half-wave ($\lambda/2$) plate and a calcite Glan Taylor air-gap polarizer (P_1 and P_2). The polarizers were oriented 45° with respect to each other. The $\lambda/2$ plates were adjusted to generate a 50-mW pump beam and a 10-mW probe beam. The beams were recombined and focused in a co-propagating noncollinear geometry with a 10-cm focal length BK-7 plano-convex lens into the sample, which was contained in a 2-mm path length, UV-grade fused-silica cell. After passing through the sample, the pump beam was blocked and the probe beam was directed to another calcite Glan-Taylor air-gap polarizer (P_3), which served as the analyzer polarizer. To reduce the stray light scattered from the pump beam, the probe beam was spatially filtered, collimated, and steered into a red-sensitive Hamamatsu S2386-8K Si photodiode placed ~2 m away from the sample region of the apparatus. The spatial filter consisted of two 5-cm focal length lenses and a 100-μm pinhole. The output of the photodiode was fed into a Stanford Research Systems SR530

lock-in amplifier that was referenced to ~5 kHz, corresponding to the sum of the frequencies of the mechanical chopper modulating the probe and pump beams. The signal was recorded and stored in a microcomputer for each position of the delay line. The signal in this homodyne configuration is quadratic in the material response.

To obtain a signal with high signal-to-noise (S/N) ratio that is linear in the material response, optical-heterodyne detection was used. In this technique, an achromatic quartz zeroth-order quarter-wave ($\lambda/4$) plate was placed between the focusing lens before the sample and polarizer P_1. With the pump beam blocked and the sample in place, the $\lambda/4$-plate was adjusted to minimize the total static birefringence along the optical train of the probe beam. For the OHD-RIKES measurements, the input polarizer, P_1, was rotated by $\leq 2°$ to obtain a local oscillator field, 90° out-of-phase with respect to the probe field. The out-of-phase heterodyned signal probes the real part of the effective nonlinear susceptibility. In principle, scans involving oppositely sensed local oscillator fields must be taken in order to correct for the residual homodyne component.[24,25] However, we could not detect this residual component in the homodyne configuration. In the analysis of the OHD-RIKES time-domain data, we assumed minimal contamination of the signal by the homodyne component.

The second-order background-free pulse intensity autocorrelation, $G_0^{(2)}(t)$, was measured by redirecting and focusing the pulses into a 100-μm KDP crystal. The same focusing lens as the lens in front of the sample was used. A photomultiplier tube was used to detect the autocorrelation signal. The pulse autocorrelation was symmetrical and well fitted by a sech^2 function even after passing through the dispersive optics in the apparatus.

OHD-RIKES signals for these ionic liquids were extremely weak (≈300 times smaller than the CS_2 nuclear response). Extensive signal averaging was required to obtain data with a S/N ratio of at least 10:1 in the nuclear part of the OHD-RIKES response. Each data set was an average of 20 scans. Each scan took 30 min to obtain. Scans were taken from −1 to +8 ps. The baseline before zero-time delay was subtracted from the data, and the data were then normalized prior to fitting the data. The signal-averaged data were fitted to model response functions with a nonlinear least-squares fitting program. Spectral densities were obtained by performing a fast Fourier transform on the data, as described previously[22] using the plotting/analysis program, Origin (Microcal).

III. Experimental Results

The response obtained in NLO time-domain experiments results from the interaction of the femtosecond laser pulse with molecules of the liquid through the third-order nonlinear polarizability. In OHD-RIKES, the interaction produces a transient birefringence in the liquid. The birefringent response of the liquid has an instantaneous component (the coherent spike), due to the electronic hyperpolarizability, and a non-instantaneous nuclear component. The non-instantaneous component is directly related to the collective polarizability anisotropy correlation function.[26] The normalized OHD-RIKES responses for C2, C4−C6, C8, and C10 are plotted in Figure 2.

Near zero-delay, the OHD-RIKES response for these RTILs is dominated by the instantaneous electronic response. The nuclear response, which appears as a shoulder on the electronic response, becomes smaller with increasing alkyl chain length. In this respect, the OHD-RIKES response is very similar to that of the normal alcohols.[26,27] The nuclear response for C10 is apparently too weak to observe with the same signal averaging used for the other liquids. For C2, C4, C5, C6, and C8, the rising edge of the pulse autocorrelation closely matches the rising edge of the OHD-RIKES signal. The signal rapidly decays, slightly lagging behind the pulse autocorrelation. At about ≈15−20% of the peak height, the signal evolves into a shoulder, which is then followed by a nonexponential decay after 500 fs (Figures 2 and 3). The nonexponential decay is characterized by a fast component and a slow component.

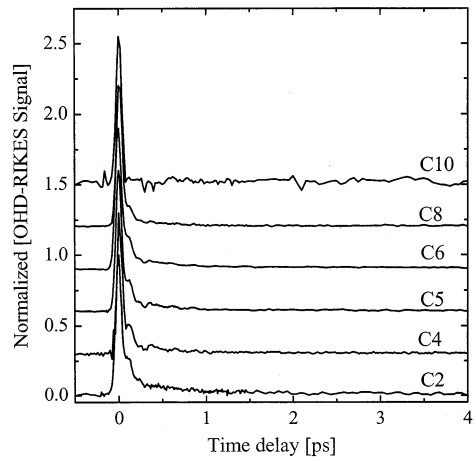

Figure 2. Normalized OHD-RIKES signals for C2, C4, C5, C6, C8, and C10 at room temperature and ambient pressure. Signals are offset in order to better show the differences.

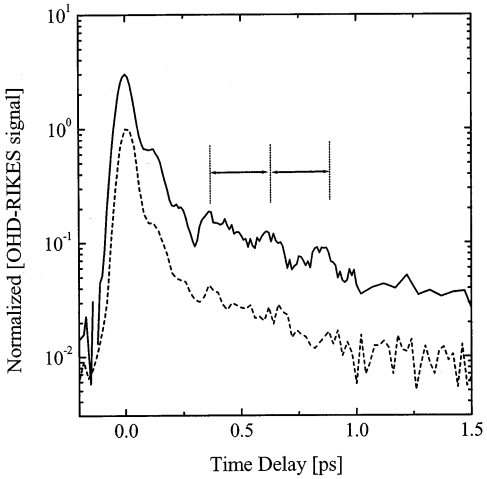

Figure 3. Semilogarithmic plot comparing OHD-RIKES responses for C5 (solid curve) and C8 (dashed curve) at short times ($t \leq 1.5$ ps). The vertical lines above the OHD-RIKES for C5 indicate the 230-fs-period oscillation.

Superimposed on the OHD-RIKES responses of C4, C5, and C6 is a coherent oscillation with a ~230 fs period. This oscillation is most noticeable for C5 (Figure 3). The oscillation persists for 3−4 periods before dropping below the noise level. The period corresponds to a frequency of ~140 cm^{-1}. These oscillations do not appear in the OHD-RIKES responses of the other RTILs. Oscillations are commonly seen in the OHD-RIKES responses of small-molecule liquids using sub-50-fs pulses. The underdamped high-frequency oscillations are normally assigned to intramolecular vibrational modes of the molecule.[25,27−32] The highly damped low-frequency oscillations, as observed for example, in pyridine,[33] benzene,[22,34] triacetin,[35] and formamide,[36] are assigned to intermolecular vibrational modes. The highly damped nature of the 140 cm^{-1} oscillation is consistent with it being due to an intermolecular vibration.

IV. Analysis and Discussion

A. Temporal Response. For pump, probe, and local oscillator pulses derived from a single transform-limited optical pulse, the OHD-RIKES signal is the convolution of $G_0^{(2)}(t)$ and the nonlinear impulse response, $R(t)$:

$$T(\tau) = \int_{-\infty}^{\infty} G_0^{\,2}(t)\, R(\tau - t)\, \mathrm{d}t \tag{1}$$

The impulse response, for optical pulses far from an electronic resonance, is given by the sum of an electronic response function, $r_e(t)$, and a nuclear response function, $r_{nuc}(t)$:

$$R(t) = r_e(t) + r_{nuc}(t) \tag{2}$$

If the electronic response is instantaneous on the time scale of the laser pulse, $r_e(t)$ can be represented by a δ-function:

$$r_e(t) = A_e \delta(t) \tag{3}$$

where A_e is proportional to the electronic hyperpolarizability. For simple molecular liquids, the long-time tail of the nuclear response is associated with diffusive dynamics arising from collective reorientation. The short time behavior of nuclear response is mainly associated with nondiffusive dynamics arising from the intermolecular vibrational motions. If the diffusive and vibrational parts of the response are assumed to be separable, the nuclear response can be represented by a sum of two terms:

$$r_{nuc}(t) = r_{vib}(t) + r_{diff}(t) \tag{4}$$

The diffusive part of the response is commonly represented by the function

$$r_{diff}(t) = A_{diff} \exp(-t/\tau_{diff})[1 - \exp(-2t/\beta)] \tag{5}$$

The $\beta/2$ rise time takes into account the fact that nuclear responses cannot follow the intensity profile of short pulses. The intermolecular response obtained by removing the diffusive part from the total nuclear response is characterized by a delayed rise ($\sim$150 fs) and a rapid Gaussian-like decay, followed by a pseudo-exponential decay with a subpicosecond 1/e time.[20,28,35,37−44] In the literature, this last feature is referred to as the "intermediate" response.

The interpretation of the intermolecular response of a simple molecular liquid is often based on a multimode curve-fitting procedure.[20−22,28,35,37−39] In this procedure, the various features of the response are assigned to different nuclear motions. The fast Gaussian-like decay is assumed to arise from librational motions. It was first suggested that the intermediate response in molecular liquids, by analogy with similar responses observed in rare gas atomic liquids,[45] originates from "interaction-induced" (or "collision-induced") effects described in the light scattering literature.[46] In another study it was suggested that the intermediate response originates from a field-induced local translational anisotropy that decays on the time scale of the density fluctuations.[28] Recent temperature-dependent studies of simple symmetric top liquids, however, have shown that the 1/e time of the pseudo-exponential tail correlates with the collective orientation time.[41] This correlation suggests that the intermediate response arises from motional narrowing and not from interaction-induced effects. Clearly, the molecular origin of the subpicosecond intermediate response is still unresolved, and there is not yet a rigorous basis for making specific assignments. The main advantage of using the multimode procedure is that it provides a quantitative framework for describing the data.

TABLE 2: OHD-RIKES Biexponential Fit Parameters[a−c]

liquid	A_f	τ_f/ps	A_s	τ_s/ps
C2	0.030	0.47	0.006	12.6
C4	0.020	0.50	0.002	8.98
C5	0.049	0.30	0.001	8.8
C6	0.042	0.29	0.003	8.5
C8	0.050	0.20	0.003	8.4

[a] See eq 6 for definition of parameters. [b] Fits were obtained for 0.5 ps $< t <$ 8 ps.

Recently, a quantum-mechanical harmonic oscillator (HO) model based on a single vibrational coordinate was shown to accurately predict the characteristic features of the intermolecular vibrational response function in neat CS_2 and its binary solutions in alkane solvents in a self-consistent fashion.[47] The fast Gaussian-like initial decay and slower pseudo-exponential decay are indications of inhomogeneously broadened intermolecular dynamics. In this model, the vibrational response is determined by just three parameters: the vibrational dephasing rate Γ and the characteristic frequency ω_0 and width σ of the frequency distribution. It was shown that the broadening of the temporal response and decrease in the prominence of the Gaussian-like contribution with increasing dilution could be accounted for by a decrease in the value of ω_0 with the values of Γ and σ relatively unchanged. The quantum HO model in principle provides an alternate framework for quantitatively describing the data.

The universal features of the intermolecular vibrational contribution to the OHD-RIKES responses of these RTILs are clearly evident (Figures 2 and 3). Because the amplitude of the vibrational component is larger than that of the diffusive component for $t < 1.5$ ps, the quasi-exponential tail of the intermolecular response can be easily seen in a semilogarithmic plot of the data (Figure 3). In this preliminary study, we will use the multimode curve-fitting procedure to obtain an initial understanding of the dynamics of these RTILs. Because of the complex short-time dynamics, it is difficult to use the full multimode curve-fitting procedure to analyze the OHD-RIKES response of these RTILs. Furthermore, because of the low S/N ratio in the long-time tails, removing the diffusive response may lead to unreliable values for the 1/e time for the tail of the intermolecular response. So instead, we fitted a biexponential decay function

$$R(t) = A_f \exp(-t/\tau_f) + A_s \exp(-t/\tau_s) \tag{6}$$

to the data between 0.5 and 8 ps using nonlinear least squares. The fits were started at 0.5 ps to avoid the initial Gaussian-like decay. It is assumed that the fast component gives the 1/e time for the tail of the intermolecular response. Fit parameters are given in Table 2, with a typical fit of the data for C5 shown in Figure 4.

The value of τ_f decreases from 0.50 to 0.20 ps in going from C4 to C8 (Table 2). However, for C2, $\tau_f = 0.47$ ps, which is less than the value that one would predict on the basis of the behavior of C4 to C8. The variation of τ_f for C4 to C8 is consistent with the hydrodynamic model for vibrational dephasing.[48] In this model, the vibrational dephasing rate is determined by the collision rate, which in turn is proportional to the viscosity. In going from C4 to C8, the viscosity increases (Table 1). Hence, vibrational dephasing should be faster in C8 than in C4, because C8 is a more viscous liquid than C4. This behavior is different than what is found for simple molecular liquids. For simple molecular liquids, the 1/e time of the pseudo-exponential tail of the vibrational response increases with viscosity.[41]

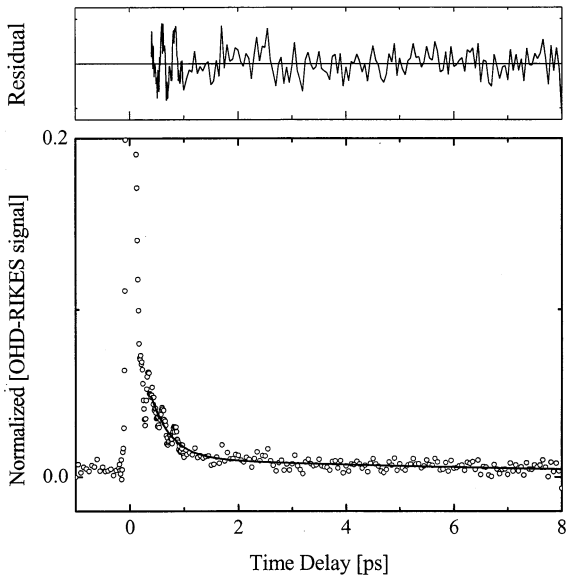

Figure 4. Typical fit of the OHD-RIKES data for C5 between 0.5 and 8 ps to a biexponential decay function (eq 6). See Table 2 for fit parameters.

B. Spectral Response. The data can be represented in the frequency-domain by using the model-independent Fourier transform procedure.[20,22,24−27,30,31,33−36,40,43,49−52] In this procedure, the OHD-RIKES response is characterized by a frequency response function

$$D(\Delta\omega) \equiv \mathcal{F}\{R(t)\} \tag{7}$$

where $\Delta\omega$ is the frequency relative to the laser center frequency and $\mathcal{F}$ denotes a forward complex Fourier transform operation. $D(\Delta\omega)$ is obtained by the complex division of the Fourier transform of the OHD-RIKES signal $T(\tau)$ by the Fourier transform of the pulse autocorrelation:

$$D(\Delta\omega) = \mathcal{F}\{T(\tau)\}/\mathcal{F}\{G_0^{(2)}(t)\} \tag{8}$$

The imaginary part, Im $D(\Delta\omega)$, gives the spectral density of the liquid. The reduced spectral density, Im $D'(\Delta\omega)$, is obtained by subtracting the long-time tail from the total OHD-RIKES signal prior to taking the Fourier transform. The reduced spectral density at low frequencies is directly related to the low-frequency Bose-corrected depolarized Raman spectrum, which arises from the intermolecular modes of the liquid.[51]

Reduced spectral densities were obtained for all of the ionic liquids, except for C10. Figure 5 illustrates the normalized spectra for C2, C4, C5, C6, and C8. For C4, C5, C6, and C8, the mean frequency is 75 ± 5 cm^{-1} and the mean full-width-half-maximum (fwhm) is 122 ± 1 cm^{-1}. The reduced spectral density for C2 has a maximum at a slightly lower frequency and is noticeably narrower than the reduced spectral densities for the other ionic liquids. The reduced spectral density of C2 has a maximum at 70 ± 5 cm^{-1} and a fwhm of 100 ± 1 cm^{-1}.

The reduced spectral densities for these liquids appear to be composed of at least two overlapping bands. This is most evident for C4, where there is a dip in the middle of the spectrum (Figure 5). Changes in the reduced spectral densities occur primarily because of changes in the relative contributions of the low- and high-frequency bands. To provide a more quantitative description of this bimodal behavior, nonlinear least-squares fits of the reduced spectral densities to various line shape functions were carried out. The best fits obtained from this analysis are shown in Figure 5 with fit parameters given in Table 3. We find that

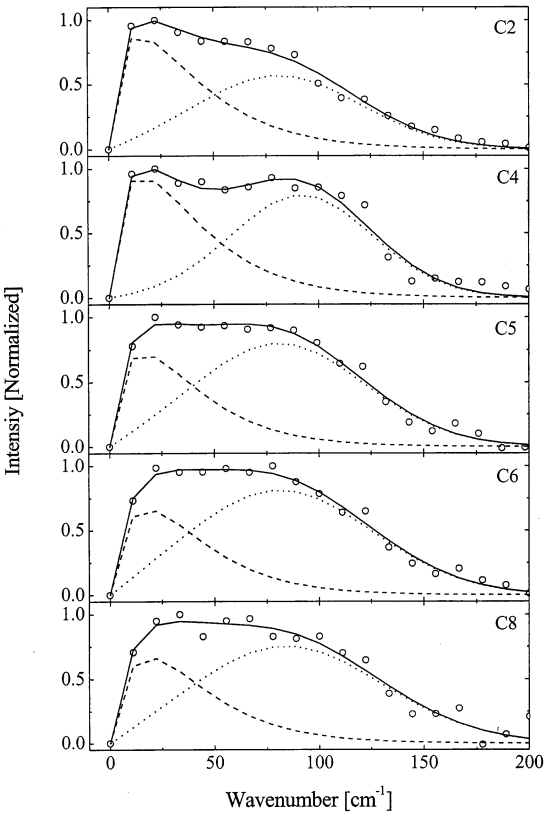

Figure 5. Reduced spectral densities for C2, C4, C5, C6, and C8 with fits to the superposition model (eqs 9−11). The solid curve in each plot is given by the sum of the Bucaro−Litovitz function (dashed curve) and the antisymmetrized Gaussian function (dotted curve). See Table 3 for fit parameters.

TABLE 3: Line Shape Parameters for Fit of Reduced Spectral Densities[a,b]

liquid	A_{BL}	a	ω_1/cm^{-1}	A_G	ω_2/cm^{-1}	ϵ/cm^{-1}
C2	0.31	0.61	24	0.57	81	39
C4	0.26	0.71	23	0.79	92	34
C5	0.17	0.77	21	0.80	81	41
C6	0.13	0.87	21	0.81	81	45
C8	0.12	0.90	21	0.75	84	47

[a] See eqs 9−11 for definition of fit parameters. [b] Fits were obtained for $0 \le \Delta\omega \le 200$ cm^{-1}.

the reduced spectral densities are well described by the sum of two bands:

$$\mathrm{Im}[D'(\Delta\omega)] = I_{BL}(\Delta\omega) + I_G(\Delta\omega) \tag{9}$$

where $I_{BL}(\Delta\omega)$ is the Bucaro−Litovitz line shape function,

$$I_{BL}(\Delta\omega) = A_{BL}(\Delta\omega)^a \exp(-\Delta\omega/\omega_1) \tag{10}$$

and $I_G(\Delta\omega)$ is the antisymmetrized Gaussian line shape function

$$I_G(\Delta\omega) = A_G\{\exp[-(\Delta\omega - \omega_2)^2/2\epsilon^2] - \exp[-(\Delta\omega + \omega_2)^2/2\epsilon^2]\} \tag{11}$$

This superposition model has been used previously to describe the reduced spectral densities for simple molecular liquids.[40,53,54] The line shape function $I_{BL}(\Delta\omega)$ was originally introduced to account for collision-induced contributions to the depolarized Rayleigh scattering (DRS) spectra of liquids.[55,56] In this study, we are not assigning any physical meaning to $I_{BL}(\Delta\omega)$. We are only using it as a fitting function.

On the basis of this superposition model, the reduced spectral densities for these liquids are characterized by a low-frequency band with a maximum at ~22 cm^{-1} and a high-frequency band with a maximum at ~84 cm^{-1}. In going from C2 to C8, the width of the low-frequency band decreases from ~56 to ~44 cm^{-1}, whereas the width of the high-frequency band increases from ~89 to ~110 cm^{-1}. Comparing the areas underneath the bands, we find that the percent contribution of the high-frequency band to the reduced spectral density increases from 55% for C2 to 61% for C5. At this point, the spectra stop changing, and the high-frequency component stays at 61−62% for C6 and C8.

These changes primarily appear to be due to intermolecular and not intramolecular effects arising from the torsional motions of the alkyl chains. This can be seen by comparing the low-frequency spectra of normal alcohols to that of the RTILs. Although OHD-RIKES data have been obtained for the alcohols,[26,27] the data do not provide sufficient resolution to obtain information about the role of the torsional dynamics of the alkyl chains in the spectra. High-resolution DRS data[57] however have been obtained for normal alcohols. The wings of the DRS intensity in these alcohols can be fitted by the equation

$$I_{DRS}(n,\Delta\omega) = A(n)\exp(-\Delta\omega/\omega_0) + \sum_{m=1}^{n} C(n,m)\exp(-\Delta\omega/\omega_m) \quad (12)$$

where n is the number of carbon atoms. The exponentials in the sum are associated with the internal rotational degrees of freedom that increase as the number of carbon atoms increases in the alkyl chain. The first term, which corresponds to the broad quasi-exponential background that accounts for 30% of the total light scattering intensity, has a value of $\omega_0 = 29$ cm^{-1}. The terms in the sum are much lower in frequency and correspond to values of ω_m, $m = 1-5$, equal to 2.7, 0.55, 0.19, 0.10, and 0.053 cm^{-1}, respectively. $I_{DRS}(\Delta\omega)$ and Im $D(\Delta\omega)$ are related to each other by the equation[25,26,35,36]

$$\mathrm{Im}[D(\Delta\omega)] = I_{DRS}(\Delta\omega)[1 - \exp(-\hbar\Delta\omega/k_BT)] \quad (13)$$

where $1 - \exp(-\hbar\Delta\omega/k_BT)$is the Bose factor. In the high-temperature limit ($\hbar\omega \ll k_BT$), eq 13 reduces to

$$\mathrm{Im}[D(\Delta\omega)] \propto \Delta\omega I_{DRS}(\Delta\omega) \quad (14)$$

At 298 K, this approximation is valid for frequencies less than $k_BT/hc \sim 207$ cm^{-1}. Thus each term in the Bose-corrected DRS spectrum represented by eq 12 is analogous to a Bucaro−Litovitz line shape function (eq 10) with the parameter a set equal to 1. The low-frequency terms associated with torsional motions of the alkyl chains are clearly absent in the reduced spectral densities of the RTILs. Interestingly, however, the frequency of the first term in eq 12 is similar to the low-frequency component given by the Bucaro−Litovitz function in the reduced spectral densities of the RTILs (Table 3).

The reduced spectral densities for RTILs are higher in frequency and broader, and slightly more structured than those of simple molecular liquids. For molecular liquids, a high-frequency reduced spectral density usually indicates a high degree of association or local order in the liquid. A high degree of association or local order results in steeper intermolecular potentials and therefore higher frequency vibrations. Water and ethylene glycol, which are highly associated molecular liquids, have bimodal reduced spectral densities that extend from 0 to 300 cm^{-1}.[35] A similar trend is observed for the reduced spectral densities for amides.[36] Dimethylformamide, an aprotic solvent, has a reduced spectral density that is given by a single band with a maximum at ~50 cm^{-1} and that extends from 0 to 150 cm^{-1}. In contrast, formamide, a protic solvent, has a reduced spectral density that extends from 0 to 300 cm^{-1} and is composed of three bands.

We think that the increase in the width of the high-frequency component in going from C2 to C8 is also an indication of increasing order in the liquid. The phase properties of RTILs suggest that increasing the length of the alkyl chain length increases the order in RTILs. Dialkylimidazolium tetrafluoroborate and hexafluorophosphate salts prepared with short alkyl chains ($n = 2-10$) are liquids at room temperature, whereas those prepared with longer alkyl chains exhibit thermotropic liquid crystalline mesomorphism.[9,58] The pattern of increasing spectral width with increasing order is also observed in molecular liquids. For example, the reduced spectral densities for methanol and ethanol are slightly broader than those of longer-chain alcohols because of the more extensive hydrogen bonding in methanol and ethanol.[26,27] The increase in the relative contribution of the high-frequency component band to the total band in going from C2 to C5 is also consistent with increased order in the liquid.

The appearance of the 140 cm^{-1} coherent oscillation in the temporal OHD-RIKES response for C4−C6 is likely to be the result of locally ordered domains in the liquid. In principle, this oscillation should appear as a peak in the spectral densities of these RTILs. However, the amplitude of the oscillation may not be sufficiently high enough to appear as a peak in the reduced spectral density data. Similar intermolecular features can be found in the light scattering spectra of molten alkali halide salts[59−66] and molten alkaline-earth halide salts [65,67,68] They appear as peaks in the wings of the spectra of molten salts. The vibrations associated with these non-central peaks are clearly not intramolecular. These peaks are thought to arise from the phonon modes of local domains with structures similar to that of the solid. The peaks occur roughly in the same region where peaks occur in the solid-state spectrum.[60,63,67,68]

V. Concluding Remarks

The dynamics of these ionic liquids are complex and do not correlate systematically with structure and bulk physical properties in a simple way. For example, it is not obvious why the OHD-RIKES response for C2 is different than those of the other five liquids. Then there is the question of the source of the 140 cm^{-1} oscillations in OHD-RIKES responses of C4, C5, and C6. Nuclear motions associated with this oscillation would have to be the result of locally ordered domains with steep intermolecular potentials that are unique to these specific RTILs. Finally, the physical origins of the low-frequency and high-frequency components of the reduced spectral densities must also be determined. We hope to address these issues in our labs by obtaining OHD-RIKES data with good S/N ratio for RTILs with anions other than the bis(triflyl)imide anion. Changing the anion should alter the local structure and therefore the intermolecular dynamics.

Because of the poor S/N ratio in the long-time tails of the data, we were unable to extract information about the diffusive response. We can roughly estimate the time scale for orientational relaxation in these systems by using dielectric spectroscopic data. Dielectric spectroscopic data for RTILs are sparse and limited mainly to highly viscous systems near the glass transition. Recently, data for the normal fluid region were obtained for room-temperature molten EAN.[15] The dielectric

relaxation time for EAN was found to vary from 130 ps at 308 K to 180 ps at 288 K. This dielectric relaxation time is primarily associated with the reorientational motion of the $C_2H_5NH_3^+$ ion. The viscosity of EAN is comparable to the viscosities of C2−C8. Therefore, because dialkylimidazolium and NTf_2^- ions are larger than the $C_2H_5NH_3^+$ ion, the orientational times in C2−C8 clearly should be greater than 200 ps. The values of τ_s are too small, on the basis of the size of the ions and viscosity. The values of τ_s also decrease with viscosity, which is not in accord with diffusive behavior as predicted by the Debye−Stokes−Einstein equation.[69−71] Therefore, we cannot assign any physical significance to the values of τ_s obtained from these data.

The lack of knowledge of the diffusive response does not prevent us from obtaining reduced spectral densities for these systems. At worst, it might cause some inaccuracy in the reduced spectral densities near zero frequency. It should, however, not affect the arguments presented above for the role of order in the liquid, because they are based on the high-frequency component of the reduced spectral densities. No doubt, knowledge of the diffusive response is crucial to obtaining a better understanding of the liquid-state dynamics of RTILs. In principle, information about the reorientational dynamics of these liquids and the torsional dynamics of the alkyl chains are contained in the diffusive response. Ongoing improvements in the detection sensitivity of our apparatus, the use of longer pulses (10−100 ps), and longer optical delays (up to 1 ns) will allow us in the future to study the diffusive response.

Acknowledgment. This research was supported by grants to E.L.Q. from the Robert A. Welch Foundation (D1019) and to R.A.B. from the Texas Higher Coordinating Board Advanced Research Program.

References and Notes

(1) Welton, T. *Chem. Rev.* **1999**, *99*, 2071.
(2) Wasserscheid, P.; Keim, W. *Angew. Chem., Int. Ed. Engl.* **2000**, *39*, 3772.
(3) Chun, S.; Dzyuba, S. V.; Bartsch, R. A. *Anal. Chem.* **2001**, *73*, 3737.
(4) Carmichael, A. J.; Hardarce, C.; Holbrey, J. D.; Seddon, K. R.; Nieuwenhuyzen. *Proc. Electrochem. Soc.* **2000**, *99*−*41*, 209.
(5) Larsen, A. S.; Holbrey, J. D.; Tham, F. S.; Reed, C. A. *J. Am. Chem. Soc.* **2000**, *122*, 7264.
(6) Carmichael, A. J.; Hardarce, C.; Holbrey, J. D.; Nieuwenhuyzen, M.; Seddon, K. R. *Anal. Chem.* **1999**, *71*, 4572.
(7) Bonhôte, P.; Dias, A.-P.; Papageorgiou, N.; Kalyanasundaram, K.; Grätzel, M. *Inorg. Chem.* **1996**, *35*, 1168.
(8) Fannin, A. A. J.; Floreani, D. A.; King, L. A.; Landers, J. S.; Piersma, B. J.; Stech, D. J.; Vaughn, R. L.; Wilkes, J. S.; Williams, J. L. *J. Phys. Chem.* **1989**, *88*, 2614.
(9) Holbrey, J. D.; Seddon, K. R. *J. Chem. Soc., Dalton Trans.* **1999**, 2133.
(10) Dzyuba, S. V.; Bartsch, R. A. *ChemPhysChem* **2002**, *3*, 161.
(11) Maroncelli, M. *J. Mol. Liq.* **1993**, *57*, 1.
(12) Madden, P. A.; Wilson, M. *Chem. Soc. Rev.* **1996**, *25*, 339.
(13) Fannin, A. A. J.; King, L. A.; Levisky, J. A.; Wilkes, J. S. *J. Phys. Chem.* **1984**, *88*, 2609.
(14) Gordon, C. M.; McLean, A. J. *J. Chem. Soc., Chem. Commun.* **2000**, 1395.
(15) Weingärtner, H.; Knocks, A.; Schrader, W.; Kaatze, U. *J. Phys. Chem. A* **2001**, *105*, 8646.
(16) Maroncelli, M.; Kumar, V. P.; Papazyan, A. *J. Phys. Chem.* **1993**, *97*, 13.
(17) Cho, M.; Rosenthal, S. J.; Scherer, N. F.; Ziegler, L. D.; Fleming, G. R. *J. Chem. Phys.* **1992**, *96*, 5033.
(18) Castner, E. W. J.; Maroncelli, M. *J. Mol. Liq.* **1998**, *77*, 1.
(19) Dzyuba, S. V.; Bartsch, R. A. *J. Heterocycl. Chem.* **2001**, *38*, 265.
(20) Quitevis, E. L.; Neelakandan, M. *J. Phys. Chem.* **1996**, *100*, 10005.
(21) Neelakandan, M.; Pant, D.; Quitevis, E. L. *Chem. Phys. Lett.* **1997**, *265*, 283.
(22) Neelakandan, M.; Pant, D.; Quitevis, E. L. *J. Phys. Chem. A* **1997**, *101*, 2936.
(23) Asaki, M.; Huang, C. P.; Garvey, D.; Zhou, J.; Kapteyn, H. C.; Murnane, M. M. *Opt. Lett.* **1993**, *18*, 977.
(24) Palese, S.; Schilling, L.; Miller, R. J. D.; Staver, P. R.; Lotshaw, W. T. *J. Phys. Chem.* **1994**, *98*, 6308.
(25) Lotshaw, W. T.; McMorrow, D.; Thantu, N.; Melinger, J. S.; Kitchenham, R. *J. Raman Spectrosc.* **1995**, *26*, 571.
(26) Cho, M.; Du, M.; Scherer, N. F.; Fleming, G. R.; Mukamel, S. *J. Chem. Phys.* **1993**, *99*, 2410.
(27) Kinoshita, S.; Kai, Y.; Ariyoshi, T.; Shimada, Y. *Int. J. Mod. Phys. B* **1996**, *10*, 1229.
(28) McMorrow, D.; Lotshaw, W. T.; Kenney-Wallace, G. A. *IEEE J. Quantum Elect.* **1988**, *24*, 443.
(29) McMorrow, D. *Opt. Commun.* **1991**, *86*, 236.
(30) Deuel, H. P.; Cong, P.; Simon, J. D. *J. Phys. Chem.* **1994**, *98*, 12600.
(31) Vöhringer, P.; Scherer, N. F. *J. Phys. Chem.* **1995**, *99*, 2684.
(32) Bartolini, P.; Ricci, M.; Torre, R.; Righini, R.; Santa, I. *J. Chem. Phys.* **1999**, *110*, 8653.
(33) McMorrow, D.; Lotshaw, W. T. *Chem. Phys. Lett.* **1990**, *174*, 85.
(34) McMorrow, D.; Lotshaw, W. T. *Chem. Phys. Lett.* **1993**, *201*, 369.
(35) Chang, Y. J.; Castner, E. W. J. *J. Chem. Phys.* **1993**, *99*, 7289.
(36) Chang, Y. J.; Castner, E. W. J. *J. Phys. Chem.* **1994**, *98*, 9712.
(37) Kalpouzos, C.; McMorrow, D.; Lotshaw, W. T.; Kenney-Wallace, G. A. *Chem. Phys. Lett.* **1988**, *150*, 138.
(38) Kalpouzos, C.; McMorrow, D.; Lotshaw, W. T.; Kenney-Wallace, G. A. *Chem. Phys. Lett.* **1989**, *155*, 240.
(39) Chang, Y. J.; Castner, E. W. J. *J. Chem. Phys.* **1993**, *99*, 113.
(40) Chang, Y. J.; Castner, E. W. J. *J. Phys. Chem.* **1996**, *100*, 3330.
(41) Loughnane, B. J.; Scodinu, A.; Farrer, R. A.; Fourkas, J. T. *J. Chem. Phys.* **1999**, *111*, 2686.
(42) Steffen, T.; Meinders, N. A. C. M.; Duppen, K. *J. Phys. Chem. A* **1998**, *102*, 4213.
(43) McMorrow, D.; Lotshaw, W. T. *J. Phys. Chem.* **1991**, *95*, 10395.
(44) McMorrow, D.; Lotshaw, L. T. *Chem. Phys. Lett.* **1991**, *178*, 69.
(45) Greene, B. I.; Fleury, P. A.; Carter, H. L. J.; Farrow, R. C. *Phys. Rev. A* **1984**, *29*, 271.
(46) Berne, B.; Pecora, R. *Dynamic Light Scattering*, 1st ed.; Wiley: New York, 1976.
(47) McMorrow, D.; Thantu, N.; Kleiman, V.; Melinger, J. S.; Lotshaw, W. T. *J. Phys. Chem. A* **2001**, *105*, 7960.
(48) Oxtoby, D. W. *J. Chem. Phys.* **1979**, *70*, 2605.
(49) Palese, S.; Mukamel, S.; Miller, R. J. D.; Lotshaw, W. T. *J. Phys. Chem.* **1996**, *100*, 10380.
(50) McMorrow, D.; Thantu, N.; Melinger, J. S.; Kim, S. K. *J. Phys. Chem.* **1996**, *100*, 10389.
(51) Kinoshita, S.; Kai, Y.; Yamaguchi, M.; Yagi, T. *Phys. Rev. Lett.* **1995**, *75*, 148.
(52) Cong, P.; Deuel, H. P.; Simon, J. D. *Chem. Phys. Lett.* **1995**, *240*, 72.
(53) Friedman, J. S.; Lee, M. C.; She, C. Y. *Chem. Phys. Lett.* **1991**, *186*, 161.
(54) Friedman, J. S.; She, C. Y. *J. Chem. Phys.* **1993**, *99*, 4960.
(55) Bucaro, J. A.; Litovitz, T. A. *J. Chem. Phys.* **1970**, *54*, 3846.
(56) Bucaro, J. A.; Litovitz, T. A. *J. Chem. Phys.* **1971**, *55*, 3585.
(57) Benassi, P.; Mazzacurati, V.; Nardone, M.; Ruocco, G.; Signorelli, G. *J. Chem. Phys.* **1989**, *91*, 6752.
(58) Gordon, C. M.; Holbrey, J. D.; Kennedy, A. R.; Seddon, K. R. *J. Mater. Chem.* **1998**, *8*, 2627.
(59) Clarke, J. H. R.; Woodcock, L. V. *J. Chem. Phys.* **1972**, *57*, 1006.
(60) Giergiel, J.; Eklund, P. C.; Subbaswamy, K. R. *Solid State Commun.* **1981**, *40*, 139.
(61) Mitchell, E. W. J.; Raptis, C. *J. Phys. C* **1983**, *16*, 2973.
(62) Raptis, C.; Bunten, R. A. J.; Mitchell, E. W. J. *J. Phys. C* **1983**, *16*, 5351.
(63) Giergiel, J.; Subbaswamy, K. R.; Eklund, P. C. *Phys. Rev. B* **1984**, *29*, 3490.
(64) Qiu, S. L.; Bunten, R. A. J.; Dutta, M.; Mitchell, E. W. J.; Cummins, H. Z. *Phys. Rev. B* **1985**, *31*, 2456.
(65) McGreevy, R. L. *J. Chem. Soc., Faraday Trans. 2* **1987**, *83*, 1875.
(66) Raptis, C.; Mitchell, E. W. J. *J. Phys. C* **1987**, *20*, 4513.
(67) Bunten, R. A. J.; McGreevy, R. L.; Mitchell, E. W. J.; Raptis, C.; Walker, P. J. *J. Phys. C* **1984**, *17*, 4705.
(68) Bunten, R. A. J.; McGreevy, R. L.; Mitchell, E. W. J.; Raptis, C. *J. Phys. C* **1986**, *19*, 2925.
(69) Einstein, A. *Investigations on the Theory of Brownian Motion*, 1st ed.; Dover: New York, 1956.
(70) Debye, P. *Polar Molecules*, 1st ed.; Dover: New York, 1929.
(71) Dote, J. L.; Kivelson, D.; Schwartz, R. N. *J. Phys. Chem.* **1981**, *85*, 2169.